Enhancement of spin coherence using *Q*-factor engineering in semiconductor microdisc lasers

S. GHOSH[1], W. H. WANG[2], F. M. MENDOZA[1], R. C. MYERS[1], X. LI[2], N. SAMARTH[2], A. C. GOSSARD[1] AND D. D. AWSCHALOM[1]*

[1]Center for Spintronics and Quantum Computation, University of California, Santa Barbara, California 93106, USA
[2]Materials Research Institute, Penn State University, University Park, Pennsylvania 16802, USA
*e-mail: awsch@physics.ucsb.edu

Published online: 26 March 2006; doi:10.1038/nmat1587

Semiconductor microcavities offer unique means of controlling light–matter interactions in confined geometries, resulting in a wide range of applications in optical communications[1] and inspiring proposals for quantum information processing and computational schemes[2,3]. Studies of spin dynamics in microcavities, a new and promising research field, have revealed effects such as polarization beats, stimulated spin scattering and giant Faraday rotation[4–8]. Here, we study the electron spin dynamics in optically pumped GaAs microdisc lasers with quantum wells and interface-fluctuation quantum dots[9] in the active region. In particular, we examine how the electron spin dynamics are modified by the stimulated emission in the discs, and observe an enhancement of the spin-coherence time when the optical excitation is in resonance with a high-quality ($Q \sim 5{,}000$) lasing mode. This resonant enhancement, contrary to expectations from the observed trend in the carrier-recombination time, is then manipulated by altering the cavity design and dimensions. In analogy with devices based on excitonic coherence, this ability to engineer coherent interactions between electron spins and photons may provide new pathways towards spin-dependent quantum optoelectronics.

Semiconductor microdisc lasers, based on whispering-gallery optical resonances[10], have been the subject of considerable interest, given their fast response time, scalability and in-plane emission[11]. These features make them attractive components for on-chip integration in optoelectronic devices. The fabrication of microdiscs embedded with quantum dots[12] has led to proposals of quantum computational schemes based on the mediation of interactions between distant quantum dot spins coherently coupled through a single microdisc mode[2]. In this letter, we study the coupling between the microdisc emission and the localized spins in its active region, as a first step towards using light–matter information exchange for quantum information processing schemes in a solid-state system.

Our samples are fabricated from GaAs/AlGaAs heterostructures grown by molecular beam epitaxy. Figure 1a (inset) is a scanning electron microscope (SEM) image of a representative microdisc with a diameter of approximately 4 μm. The optically active region contains five 4.2-nm-thick undoped GaAs quantum wells, separated by 10-nm-thick $Al_{0.31}Ga_{0.69}As$ barriers. The total thickness of the disc is about 110 nm, ensuring that only the lowest-order cavity modes are supported[10]. At each quantum well–barrier interface, growth interruptions of 2 min are introduced to induce monolayer fluctuations, leading to the formation of natural quantum dots. Control samples, consisting of discs of identical dimensions, are fabricated from heterostructures with the same design but with only 5-s of growth interruptions. Low-temperature microphotoluminescence measurements at low excitation power ($P_{exc} < 10$ μW) show clear, resolution-limited spectral features (full-width at half-maximum, FWHM ~ 200 μeV) only in the former samples, confirming the presence of quantum dots in the active region[13]. At higher excitation powers, both samples support whispering-gallery resonant modes, but the *Q*-factor is consistently higher in the quantum-dot samples ($Q \sim 5{,}500$) than in the control samples ($Q \sim 2{,}000$).

Spectroscopic and dynamic details of the stimulated emission at temperature $T = 5.5$ K from a microdisc with quantum dots are shown in Fig. 1. A tunable, pulsed Ti:sapphire laser, producing approximately 150-wide pulses at a repetition rate of 76 MHz, is tuned to 740 nm to optically pump the discs for photoluminescence measurements. The samples are mounted in an optical cryostat with a variable temperature insert and a 7 T superconducting magnet. The incident laser is focused to a spot approximately 30 μm in diameter at an angle of 45° to the sample normal. The photoluminescence is collected perpendicular to the excitation direction in reflection geometry. The inter-disc distance is 50 μm, allowing us to address a single structure within the laser spot. At low incident power ($P < 200$ W cm^{-2}) the emission is mostly spontaneous, with the beginnings of cavity coupling

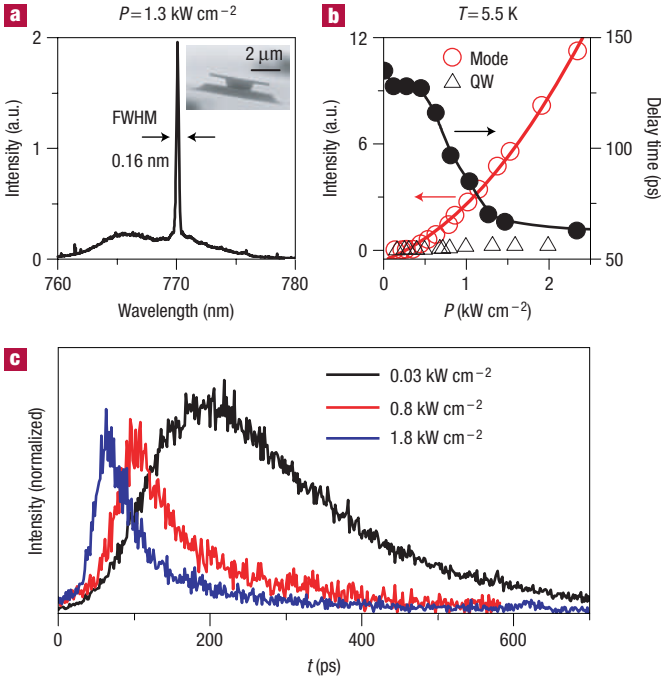

Figure 1 Static and dynamical characteristics of microdiscs. **a**, Photoluminescence spectral emission from a disc (diameter approximately 4 μm) excited by a pulsed laser at 740 nm, showing a resonant mode at 770 nm with $Q \sim 4{,}800$. Inset: SEM image of a disc. **b**, Time-integrated intensity of the resonant emission (red circles) and the spontaneous emission (black triangles) as a function of P. Fit to the mode intensity (red line) yields the lasing threshold QW = quantum well. **c**, Time-resolved emission at 770 nm with varying pump power. The delay time decreases with increasing input power, starting at the threshold, as shown in **b** (black circles).

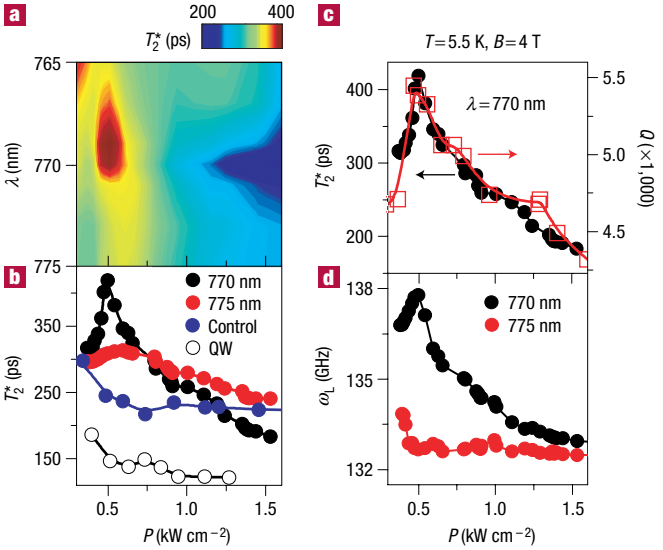

Figure 2 Resonantly enhanced spin coherence. **a**, Map of T_2^* as a function of λ and P. Spin coherence is enhanced at the lasing mode at low pump powers, and decreases as the power increases. **b**, T_2^* as a function of pump power from line-cuts across **a**, illustrating the resonant coupling at 770 nm (black). A similar line cut at 775 nm (red), off-resonance, shows no such enhancement. T_2^* in the unprocessed heterostructure (open circles), as well as in a control sample (blue), both shown here at 770 nm, remain unchanged with P. **c**, Variations in T_2^* and the cavity Q-factor at 770 nm with P. **d**, The Larmor precession frequency, ω_L, in the cavity, obtained from fits to spin precession data, as a function of P. For all the Kerr rotation measurements, the probe power is approximately 15 W cm^{-2}.

shown through the emergence of a few modes. With increasing power, one of these modes starts to dominate and the spectrum shows resonant emission at 770 nm with a transparency $Q = 5{,}500$. Figure 1a shows the photoluminescence emission of the mode at $P = 1.3$ kW cm^{-2} and Fig. 1b shows the contrast between the power dependence of the time-integrated intensities of the lasing mode and the spontaneous emission. A fit to the logarithmic plot of the mode output intensity as a function of input power[14] indicates stimulated emission with a threshold of 450 W cm^{-2}. Figure 1c shows time-resolved photoluminescence traces of the spectrally resolved lasing emission at different pump powers, taken with a streak camera (time resolution of about 2 ps). Above the threshold power, the delay time, defined as the time interval between the arrival of the laser pulse (at time $t = 0$) and the maximum of the cavity emission, starts decreasing with increasing pump power, as shown in Fig. 1b. This is another indication of the onset of stimulated emission[15].

Time-resolved Kerr rotation, an optical pump–probe spectroscopic technique[16,17], is used to probe the electron-spin dynamics in the cavities (in the Voigt geometry, detailed in the Supplementary Information, Fig. S1a). A circularly polarized pump pulse, incident on the sample surface, injects spin-polarized carriers, with the circular polarization being modulated with a photoelastic modulator at 50 kHz for lock-in detection. The spin of the optically generated hole experiences decoherence that is typically faster than that of the electron both in quantum wells[18] and in quantum dots[19]. The Kerr rotation angle of a linearly polarized probe pulse (tuned to the same wavelength as the pump) applied after a time delay Δt therefore measures the projection of the electron spin magnetization as it precesses about the applied magnetic field. We extract an inhomogeneous transverse spin lifetime, T_2^*, from the exponentially decreasing envelope of the spin-precession curve and the Larmor precession frequency, ω_L, from the transverse oscillations (see the Supplementary Information, Fig. S1b).

Figure 2a is a map of T_2^*, at $T = 5.5$ K with an applied magnetic field $B = 4$ T, as we vary both the pump wavelength (λ) and P. We immediately notice an anomaly near the lasing wavelength at $\lambda = 770$ nm. T_2^* first increases to 456 ps when $P \sim 0.5$ kW cm^{-2}, and then decreases to 158 ps as P is increased to 1.5 kW cm^{-2}. Such drastic variations in T_2^* are not observed at any other wavelengths, as shown further by the line-cuts taken at fixed λ (770 and 775 nm) and plotted in Fig. 2b. For comparison, we also plot T_2^* as a function of P for the unprocessed heterostructure (with quantum dots but no cavity) and for a resonant mode in a cavity in the control sample (no quantum dots). Neither of these shows a comparable variation of T_2^* with P as seen in the quantum-dot sample. Although this is expected in the unprocessed heterostructure, the lack of resonant enhancement in the control sample may be attributed to the lower quality of the mode.

A careful look at Fig. 2a reveals that the value of P where the increase in T_2^* occurs in the quantum-dot sample is very close to the threshold power for lasing in the disc. The lasing threshold is characterized by changes in various parameters, such as an increase in the mode output intensity, a decrease in the delay time and a change of the mode Q-factor as the system crosses over from spontaneous to stimulated emission. Plotting Q of the resonant mode (obtained from photoluminescence) as a function of P in

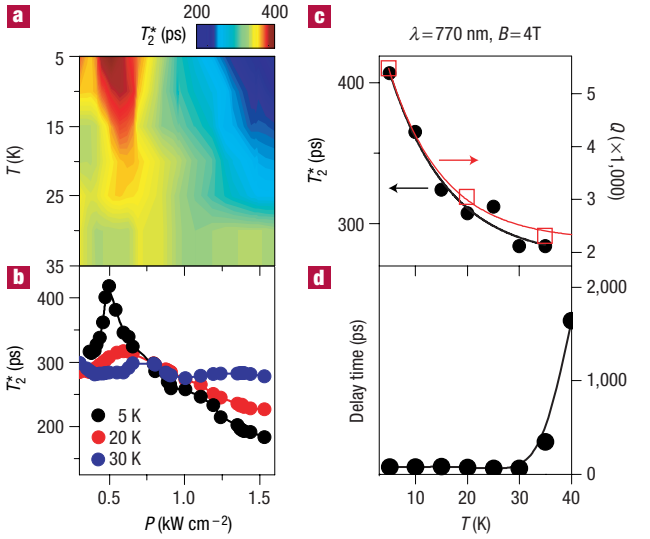

Figure 3 Temperature dependence. **a**, T_2^* as a function of T and P at the cavity resonance (770 nm). **b**, Line-cuts across **a**, at $T = 5$ K, 20 K and 30 K, showing the resonant enhancement of T_2^* diminishing with increasing T. **c**, T_2^* (black circles, $\lambda = 770$ nm, $P = 0.5$ kW cm^{-2}) decreases with T. Variation of the mode Q-factor (red squares), and of the delay time of disc emission (**d**), point to the decrease being related to the reduction of stimulated emission with increasing temperature. Lines in **c** are exponential fits.

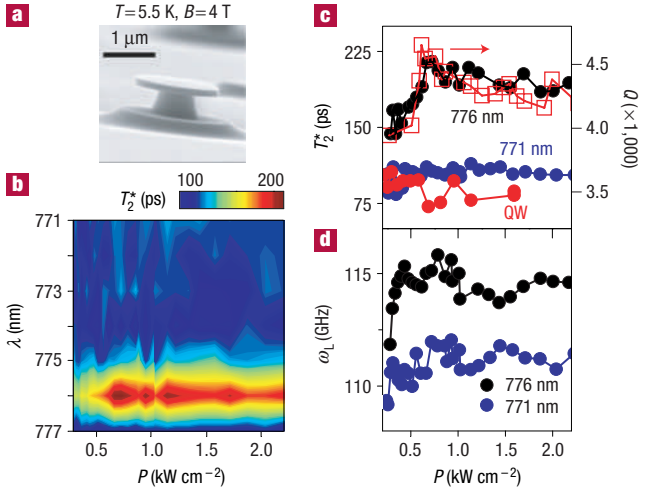

Figure 4 Robust spin-coherence enhancement in smaller cavity. **a**, SEM image of microdisc with a diameter of approximately 1.5 μm. This reduced size causes the resonance wavelength to shift to 776 nm. **b**, T_2^* as a function of λ and P. The resonant increase in T_2^* at 776 nm is robust to higher values of P. **c**, Line-cuts across **b** for 776 nm (black) and 771 nm (blue) along with the power dependence of T_2^* in the unprocessed heterostructure (red circles) and of Q (red squares). **d**, ω_L at 776 and 771 nm, showing a similar trend with P as T_2^*.

Fig. 2c shows an increase at the threshold and a subsequent decrease at higher powers. The qualitative variation of Q with P traces the evolution of the spin lifetime very well, revealing the possibility that T_2^* can be enhanced by engineering cavities with larger Q. Figure 2d shows ω_L in the quantum-dot sample at $B = 4$ T with $\lambda = 770$ and 775 nm (on and off resonance, respectively) as P is varied. It also increases at the resonant wavelength, over the same range in power as T_2^*.

In addition to varying P, we may also vary the temperature to alter the lasing characteristics of the microdisc. In Fig. 3a we map out T_2^* as a function of P at different temperatures with the pump fixed at 770 nm. The modulations in T_2^* with P decrease with temperature, disappearing by $T = 35$ K, shown by the line-cuts at three different temperatures (Fig. 3b). In Fig. 3c, we follow the change in T_2^* with temperature at $P = 0.5$ kW cm^{-2} (black) and, once again, it agrees qualitatively with the variation of the mode Q-factor (red) with temperature; both decrease exponentially. Not only is the mode quality degraded, but the emission at 770 nm is no longer dominated by stimulated emission, evident in the sharp increase in the delay time around 35 K (Fig. 3d).

Owing to the spectral overlap of the emission from the quantum wells and the quantum dots, it is not possible to unequivocally identify either as the sole source of the lasing emission in the discs. However, the samples with quantum dots have (i) consistently higher Q-factors, implying lower dissipation, and (ii) shorter delay times, resulting from less carrier diffusion to the edges. This suggests the involvement of the quantum dots, which provide confinement of the carriers and hence prevent non-radiative recombination at the sidewalls, at least under conditions of 'moderate' excitation and low temperature. As the pump power (temperature) increases, quantum-dot states saturate (depopulate) and recombination is favoured from quantum-well states. The carriers not only diffuse to the sidewalls and recombine non-radiatively, but also begin to couple extensively to radial modes, which is borne out by the photoluminescence data[13], where we see 'mode hopping': the lasing emission cascading to longer wavelengths by coupling to radial modes of second and third order (which are far more dissipative, and consequently, have lower Q) as T and P increase.

In an attempt to reduce the losses at higher excitation powers and temperature, we designed and fabricated discs with a smaller diameter (~1.5 μm). Figure 4a is an SEM image of such a disc. The chief advantage of these smaller discs is that the spectral width of the gain supports only one mode (the mode spacing of the whispering-gallery modes is inversely proportional to the radius of the disc) and should, in principle, lead to reduced losses. Photoluminescence emission from the disc consists of a single lasing mode at 776 nm, with a Q-factor that increases at low powers. However, in sharp contrast to larger discs, the Q-factor remains nearly constant at approximately 4,500 over a large power range (Fig. 4c, red squares), showing no indication of mode quality degradation or emergence of higher-order radial modes. The spin lifetime plotted in Fig. 4b shows resonant enhancement at the lasing mode, and also does not decrease with increasing power, unlike in the larger discs. It persists until the pump power is quite high (2.2 kW cm^{-2}). The line-cuts in Fig. 4c show T_2^* on and off resonance, and in the unprocessed heterostructure. T_2^* in the cavity once again follows the variation in mode Q-factor. In Fig. 4d, ω_L for two different pump wavelengths is shown and it is found to be larger on resonance than off.

We have demonstrated the possibility of increasing spin coherence at selective wavelengths in a cavity, by coupling to high-Q modes. This resonant enhancement would be of great interest in microdiscs with embedded self-assembled quantum dots, for which very high Q values have been reported[20]. At this point, we do not have an explanation for the resonant increase in the spin-coherence time or the Larmor precession frequency, although it is a clear indication of the existence of some form of coupling between the cavity emission and the carrier dynamics. However, our results show that we can engineer control over the cavity–spin coupling

by means of microcavity designs that robustly enhance the spin coherence time by reducing mode degradation. Results have shown the possibility of creating entanglement between resonant states of optically coupled discs[21] and of efficient read-out by fibre coupling to discs[22]. These advancements taken together make these systems very promising candidates for quantum information processing.

Received 16 September 2005; accepted 22 December 2005; published 26 March 2006.

References

1. Vahala, K. J. Optical microcavities. *Nature* **424,** 839–846 (2003).
2. Imamoglu, A. *et al.* Quantum information processing using quantum dot spins and cavity QED. *Phys. Rev. Lett.* **83,** 4204–4207 (1999).
3. Meier, F. & Awschalom, D. D. Spin-photon dynamics of quantum dots in two-mode cavities. *Phys. Rev. B* **70,** 205329 (2004).
4. Hallstein, S. *et al.* Manifestation of coherent spin precession in stimulated semiconductor dynamics. *Phys. Rev. B* **56,** R7076–R7079 (1997).
5. Lagoudakis, P. *et al.* Stimulated spin dynamics of polaritons in semiconductor microcavities. *Phys. Rev. B* **65,** 161310 (2002).
6. Cubian, D. P. *et al.* Photoinduced magneto-optic Kerr effects in asymmetric semiconductor microcavities. *Phys. Rev. B* **67,** 45308 (2003).
7. Martin, M. D., Aichmayr, G., Vina, L. & Andre, R. Polarization control of nonlinear emission of semiconductor microcavities. *Phys. Rev. Lett.* **89,** 077402 (2002).
8. Salis, G. & Moser, M. Faraday-rotation spectrum of electron spins in microcavity-embedded GaAs quantum wells. *Phys. Rev. B* **72,** 115325 (2005).
9. Brunner, K., Abstreiter, G., Bohm, G., Trankle, G. & Weimann, G. Sharp-line photoluminescence of excitons localized at GaAs/AlGaAs quantum well inhomogeneities. *Appl. Phys. Lett.* **64,** 3320–3323 (1994).
10. McCall, S. L., Levi, A. F. J., Slusher, R. E., Pearton, S. J. & Logan, R. A. Whispering gallery mode microdisk lasers. *Appl. Phys. Lett.* **60,** 289–291 (1992).
11. Baba, T., Inoshita, K., Sano, D., Nakagawa, A. & Nozaki, K. Microlasers based on photonic crystal concept. *Int. Soc. Opt. Eng.* **5000,** 8–15 (2003).
12. Young, D. K., Zhang, L., Awschalom, D. D. & Hu, E. L. Coherent coupling dynamics in a quantum-dot microdisk laser. *Phys. Rev. B* **66,** 081307 (2002).
13. Wang, W. H. *et al.* Static and dynamic spectroscopy of (Al,Ga)As/GaAs microdisk lasers with interface fluctuation quantum dots. *Phys. Rev. B* **71,** 155306 (2005).
14. Bjork, G., Karlsson, A. & Yamamoto, Y. Definition of a laser threshold. *Phys. Rev. A* **50,** 1675–1680 (1994).
15. Luo, K. J. *et al.* Dynamics of GaAs/AlGaAs microdisk lasers. *Appl. Phys. Lett.* **77,** 2304–2306 (2000).
16. Crooker, S. A., Awschalom, D. D., Baumberg, J. J., Flack, F. & Samarth, N. Optical spin resonance and transverse spin relaxation in magnetic-semiconductor quantum wells. *Phys. Rev. B* **56,** 7574–7588 (1997).
17. Crooker, S. A., Awschalom, D. D. & Samarth, N. Time-resolved Faraday rotation spectroscopy of spin dynamics in digital magnetic heterostructures. *IEEE J. Sel. Top. Quantum Electron.* **1,** 1082–1092 (1995).
18. Kikkawa, J. M., Smorchova, I. P., Samarth, N. & Awschalom, D. D. Room temperature spin memory in two dimensional electron gases. *Science* **277,** 1284–1287 (1997).
19. Gundogdu, K. *et al.* Electron and hole spin dynamics in semiconductor quantum dots. *Appl. Phys. Lett.* **86,** 113111 (2005).
20. Michler, P. *et al.* Laser emission from quantum dots in microdisk structures. *Appl. Phys. Lett.* **77,** 184–186 (2000).
21. Nakagawa, A., Satoru, I. & Baba, T. Photonic molecule laser composed of GaInAsP microdisks. *Appl. Phys. Lett.* **86,** 041112 (2005).
22. Srinivasan, K., Borselli, M., Johnson, T. J., Barclay, P. E. & Painter, O. Optical loss and lasing characteristics of high-quality-factor AlGaAs microdisk resonators with embedded quantum dots. *Appl. Phys. Lett.* **86,** 151105 (2005).

Acknowledgements

The authors would like to acknowledge support from DARPA/QUIST and NSF, and thank E. L. Hu, R. J. Epstein and F. Meier for illuminating discussions. Work performed in part at the UCSB and Penn State Nanofabs, members of the NSF NNIN.
Correspondence and requests for materials should be addressed to D.D.A.
Supplementary Information accompanies this paper on www.nature.com/naturematerials.

Competing financial interests

The authors declare that they have no competing financial interests.